Weili SHI, Yanfang LI, Yu MIAO, Yinlong HU

Changchun University of Science and Technology

Research on the Key Technology of Image Guided Surgery

Abstract. *It research on the key technology on IGS (image-guided surgery). It proposes medical image segmentation based on PCNN and the virtual endoscopic scenes real-time rendering method based on GPU parallel computing technology, which improves the display quality of IGS's virtual scene and real-time rendering speed. These methods are very important for IGS's applications.*

Streszczenie. *Przedstawiono technologię operacji bazującej na prowadzonym systemie obrazu IGS. Zaproponowano segmentację obrazu I możliwość otrzymywania obrazu endoskopowego w trybie czasu rzeczywistego. (**Badania możliwości technologii sterowanej obrazem operacji medycznej**).*

Keywords: Image Guided Surgery; PCNN; Medical Image Segmentation; 3D Visualization.
Słowa kluczowe: wizualizacja 3D, sterowanie operacją medyczną.

Introduction

The basic principles of IGS is to obtain CT, MRI(including other medical images) of the surgical site in patients, 3D visualization image by reconstructed. It uses the Electromagnetic Tracker System to obtain position matrix of surgical equipment and patients' coordinate system according to the World Coordinate System, it reflects the change information of surgical instruments relative to patient position into virtual real-time three-dimensional model to improve surgical accuracy and safety.

Medical image segmentation is the key technology in medical image processing and analysis, which segment the image into different regions according to the similarly and difference between the different regions. The first issue is how to segment the ROI in IGS. l Three-dimensional visualization is the key to display virtual three-dimensional model, which projected light into CT scan images using three time slinear interpolation will be projected light to generate three-dimensional model. The bottleneck of three-dimensional visualization is speeding. It will introduces the two key technologies about IGS.

Medical Image Segmentation

The research of ROI segmentation is the most important base for the medical image analysis [3]. Accurate, robust and fast image segmentation is the most important step for following steps (quantitative analysis and three dimension visualization and so on). It is also foundation for image guided surgery, radiotherapy plans and treatment evaluation and others clinical application. Medical images have the characters such as blurredness, edges and regional feature indistinctness because of physical thermal noise of imaging equipment, offset effect, partial effect, fast moving of myocardial and flowing of blood.

In the early research of medical image segmentation, it mostly directly used the classics method of image processing such as edge extraction and region growing algorithm based on gray. In recent years, with mathematics development on the theory and application. It brings the new segmentation algorithm combing with wavelet, mathematical morphology, fuzzy mathematics, genetic algorithm, neural network, Markov model, deformable model and model guide method [4, 5]. PCNN founded by Eckhorn is better than the traditional method of image processing which explains synchronization of neuron related the characteristic in the cat's brain vision cortex experiment[6]. It needs set the parameters in the mathematics model through several experiments to realize the best segmentation effect. This paper points out the automatic segmentation method for medical image based on PCNN, which can automatically set PCNN parameters. In addition, it can get the best result by the two dimension Tsallis entropy.

(A)Tsallis Entropy

As generally, entropy is the basic concept in energetic concerning with the order of irreversible process. It can be used to measure randomness in a physic system. Shannon redefined the entropy function to check the indeterminacy of information included in the system. And it quantitatively measures the amount of the information produced by a process [7].

It assumes that the system has n kinds of possible states, the possibility of each state is p= {pi}. 0≤pi≤1 and $\sum_{i=1}^{n} p_i = 1$ .And then entropy can be defined as:

$$S_{Shannon} = -\sum_{i=1}^{n} p_i \ln p_i \tag{1}$$

But its application is limited in the effective range of B-G statistical mechanics. There are many systems in the nature which can't be described by the B-G statistical mechanics, such as long-range interaction, Long-range microscopic memory (Non-markov process), Galaxies singular speed, Levy anomalous diffusion, dissipative system and so on. Therefore, Tsallis [8] brings out the Non-extensive entropy equation.

$$S_q = \frac{1 - \sum_{i=1}^{n} (p_i)^q}{q - 1} \tag{2}$$

In this equation, n is the amount of possible states of the system, q is Non-extensive parameter.

The statistical mechanics which is based on Non-extensive is called Non-extensive statistical mechanics or general statistical mechanics. B-G statistical mechanics is included in it when q approximate to 1 limitlessly.

$$S_{Shannon} = \lim_{q \to 1} S_q \tag{3}$$

As the parameter in Tsallis entropy, q describes the degree of Non-extensive. When the system consists of two independent systems A and B, the system entropy Sq(A+B) meets the following pseudo-additivity.

$$S_q(A+B) = S_q(A) + S_q(B) + (1-q)S_q(A)S_q(B) \tag{4}$$

The traditional image processes think that an image can be regarded as a Markov field. For simplify the processing, it only think the field remember adjective units. In fact, Natural image itself owns two aspect characteristics of long-range microscopic memory and dissipative system. Non-extensive Statistical mechanics can describe image itself appropriately. After processing hundreds of images, using the Non-extensive entropy (q=0. 8) is better than Shannon entropy [9].

However, after getting the histogram of image, it can work out the Tsallis entropy by the equation (2). It is better than the Shannon entropy. As the histogram considers the gray information, it easily becomes the boundary interrupted and less segmented by using the equation (2). Considering that the two dimension histogram not only includes the gray information but also spatial information, this paper combines the Tsallis entropy with two dimension histogram.

An image size is M×N. The gray-scale is L. f(x,y) describes the gray value of pixel(x, y). g(x, y) describes the neighborhood average gray value. It needs consider the boundary effect when calculating g(x,y). For example, when considering 3×3 neighborhood average gray value, it needs ignore the two rows of image both top and bottom and two columns of image both left and right. The equation of image's two dimension histogram:

$$h(m,n) = P\left\{f(x,y) = m, g(x,y) = n\right\} \tag{5}$$

It can adopt the correlation frequency method to estimate, which means h(m ,n)= numel(f(x, y)=m, g(x, y)=n)/(MN).

Supposed that image f has been segmented into the goal set O and the background set B, the image's two-dimensional Tsallis entropy is defined as [8]:

$$S_q(f) = S_q(O) + S_q(B) + (1-q)S_q(O)S_q(B) \tag{6}$$

In this equation, Sq(O) and Sq(B) correspond goal O and the background B Tsallis entropy respectively, the definitions are as follows:

$$S_q(O) = \frac{1 - \sum_{i=1}^{L}\sum_{j=1}^{L}\left[h_{ij}(O)\right]^q}{q-1} \tag{7}$$

$$S_q(B) = \frac{1 - \sum_{i=1}^{L}\sum_{j=1}^{L}\left[h_{ij}(B)\right]^q}{q-1} \tag{8}$$

(B)The basic model of PCNN

The pulse coupling neural network is an artificial neural network, which was founded in the last century 90's, completely different from artificial neural networks. Eckhorn and his colleagues found that the synchronized shake phenomenon appeared in the local areas of different positions caused by similar stimulus input [9] in the study of the cat visual cortex. Later, in the experiments on monkeys they gained the same result [10]. Then Eckhorn bring out pulse coupling neural network model. Because this model is highly nonlinearity and complex reciprocity, it is difficult to use mathematical methods to control and interpret the results of neuronal behaviour. So in 1999Johnson transformed Eckhorn's model into PCNN model [11].

Figure 1 shows a PCNN neuron model, which is made up of receive part, modulation and pulse generator parts. Its discrete mathematics equation description is as follows:

$$F_{ij}[n] = \exp(-\alpha_F)F_{ij}[n-1] + V_F\sum M_{ijkl}Y_{kl}[n-1] + I_{ij} \tag{9}$$

$$L_{ij}[n] = \exp(-\alpha_L)L_{ij}[n-1] + V_L\sum W_{ijkl}Y_{kl}[n-1] \tag{10}$$

$$U_{ij}[n] = F_{ij}[n]\left(1+\beta L_{ij}[n]\right) \tag{11}$$

$$Y_{ij}[n] = \begin{cases} 1 & U_{ij}[n] > \theta_{ij}[n-1] \\ 0 & U_{ij}[n] \le \theta_{ij}[n-1] \end{cases} \tag{12}$$

$$\theta_{ij}[n] = \exp(-\alpha_\theta)\theta_{ij}[n-1] + V_\theta Y_{ij}[n-1] \tag{13}$$

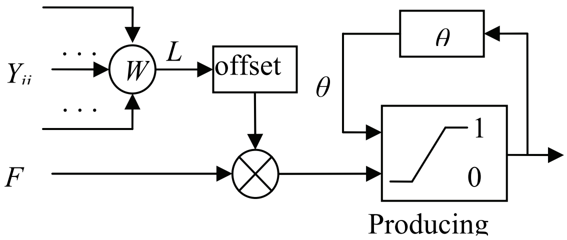

Fig.1. Neuron Model of PCNN

Equation (9) ~ (13) describes the PCNN neurons. i, j are the neuron markings, n is the iterations, I is neurons external stimulation, F is feedback input, L is connecting input, U is internal activity items, θ is dynamic threshold; M and W are connection weight matrixes (typically M = W); VF, VL, Vθ are amplitude constants for F, L, θ respectively ; VF, VL, Vθ third party αF, αL, αθ are corresponding attenuation coefficients respectively; β is connection coefficient; Y is PCNN binary output. Receive part accepts the input of others neurons or external parts, After receiving the input, the receive part transmits them through two channels. One is the F channel, the other is L channel. When PCNN is used for image processing, the input of F channel is the gray of correspond pixel, the input of L channel is the output of neighborhood neuron generally. Iij represents the gray value of corresponding pixel. After multiplying Lij from L channel adding the plus offset with the Fij from F channel, the modulation part gets the internal state Uij. Input the Uij into the pulse generation part. If Uij is bigger than θij , this neuron outputs a pulse, meanwhile, θij is increased through the feedback. On the other hand, θij is exponentially damped with the time growing.

When PCNN is used for image segmentation, it is the single two dimension local connection network. The neuron is corresponding with the pixel one by one. Each neuron is connected with the corresponding pixel which is also connected with the neighbor neuron. Input each gray value of pixel into corresponding F channel. The L channel of each neuron is connected with other neuron's output in neighborhood and receives their outputs. Each neuron only has two states, outputting pulse or not.

(C)Improved PCNN Algorithm

For the medical image processing, it is not in strict with the true nature of biological neurons. From the target and precision of the medical image segmentation, using the inhibitory properties of neurons, it adopts the search method of the traditional threshold segmentation technology, which means adopting the single increasing threshold function from smaller to bigger. It also simplifies PCNN model, as shown:

$$F_{ij}[n] = I_{ij} \tag{14}$$

$$L_{ij}[n] = V_L\sum W_{ijkl}Y_{kl} \tag{15}$$

$$E_{ij}[n] = E[n] = \begin{cases} g[n]E_0, Y_{ij}[n-1] = 1 \\ E_0, \quad Y_{ij}[n-1] = 0 \end{cases} \tag{16}$$

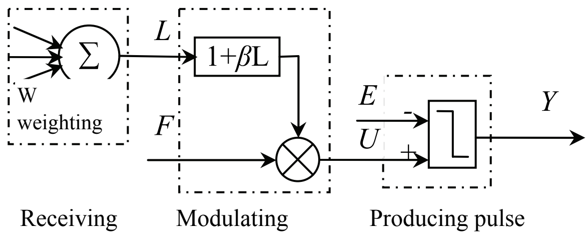

Fig.2. Improved PCNN neuron model

Using the improved PCNN model for the medical image segmentation, the neuron output is associated with the pixel value of the medical image, that is Fij[n]=Iij. Each neuron receives the neuron connection input, whose distance is within R. W that is the internal weigh coefficient matrix, and each element's value is reciprocal of Euclidean distance from the central pixel to around each pixel. G[n] is the function increasing with the time growth.

Using this algorithm for medical image segmentation, each neuron can only be activated once. Concrete steps are as follows:

1)Set the initial values of PCNN parameters, which means that all threshold values are set to be zero. The aim is that all pixels can be activated;

2)Generate the next iteration threshold according to equation (16);

3)Do the circulate iterating according to equation(14)-(16): When in the neighborhood where W(internal weight coefficient matrix) is there appears the pixel whose gray value is similar with others, and some pixel's gray value is less than the input threshold. These pixels output the pulse one by one; other around neurons whose gray values are similar can output pulse. Then produce the pulse sequence Y[n].

The output image produced by PCNN is the output sequence Y[n]. Through the principle of two dimension Tsallis entropy maximum, it makes two dimension Tsallis entropy in equation (6) is max to get the best value in the output sequence Y[n]. This value is the best segmentation result of the image.

Fig.3. Head blood vessel

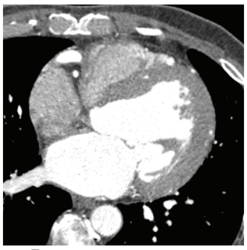

Fig.4. Bosom

(D)Simulation results analysis

In this section, All algorithms were run on a Dell OptiPlex 170L PC. This choice was motivated by the fact that a PC is much cheaper and more widely available. The PC employed in this study had a main memory of 1024 MB and one hard disk unit of 80 GB. Its CPU was an Intel Pentium IV microprocessor running at 2.8 GHz. All programs were written in the C++ programming language and were compiled under Microsoft Visual C++ 6.0 and run under Windows XP (32-bit) operating system. All image data were first stored on the hard disk.

Two data sets were employed for this paper. The first data consisted of MRI images of the human head (see Fig. 3). The images had a spatial resolution of 448×576×120 and a dynamic range of 12 bits. The second data consisted of CT X-ray images of the human bosom (see Fig. 4). The images had a spatial resolution of 512×512×355 and a dynamic range of 12 bits. Fig 3 is the MRI original image of human head. Fig 4 is the CT original image of human bosom. Fig 5 and fig 7 are the unsegmented 3D reconstruction results.Fig 6 and fig8 are the segmented results by this paper's algorithm. From the fig6 and fig8, the vessels and heart are segmented effectively, and the details are perfect.

Fig.5. The human head vessel reconstruction result

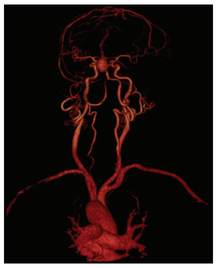

Fig.6. The segmentation result of human head blood vessel

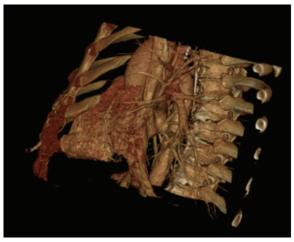

Fig.7. The human bosom reconstruction result

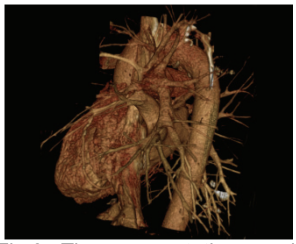

Fig.8. The segmentation result of bosom reconstruction

For medial image segmentation, this paper improves the changeable threshold function in PCNN, which combined with 2-D Tsallis entropy to segment the image automatically. As a result, this algorithm has the following advantages: the better image segmentation precision, the stronger adaptability. Especially this algorithm's superiority is obvious when the edge of image forward is faintness.

3D Visualization

At present, there are three methods for medical image data set visualization: 1) speed-up based on software. It uses the property of volume data to optimize volume algorithm. Typical algorithm includes eight tree decomposing, ray ending, Shearsarp and Spattin. 2) Speed-up based on hardware. Its idea is to Develop special hardware for real-time volume rending. Typical hardware includes VolumePro and VIZAR made by TeraRecon, which are not widely used because of the high price. 3) Speed-up based on GPU. With programmable pc widely used and CUDA appearing, programming based on PC is widespread.

(A)Ray Casting Volume Rending

In 1988, Sabella and Levoy introduced a typical volume rending algorithm based on image space sequences: Ray Casting algorithm. The main idea is to simulate the process of the light ray projecting onto some translucent object, after refraction and absorption, the reflected light ray forming an image on the opposite direction. As shown in Fig N, a light ray ds projects on the object at point a, travels between point a and b, leaves from point b. When the ray is traveling in the object, the object working on the ray is continue, which is not realized in the algorithm. It is clear that the interaction between the object particles and the beam is continuous, when the ray is traveling in the object. However, the algorithm could not accurately simulate the interaction. In practice, the continuous rays are treated as some discrete points by resampling. This method could approximately simulate the process of the light ray travels inside the object.

Assume there are particles distributed fully in a 3-dimensional data field, and assume these particles absorb completely any light beams striking in without any ray escaping. This is then the simplest ray absorption model in volume rendering. In this case, the volume rendering equation is,

(17) $$I(s) = I_0 e^{-\int_0^k \tau(t)dt}$$

where, I_0 is the lumination intensity at s=0, s is the length parameter along the direction of the ray entering, $I(s)$ is the intensity at s, τ is the light decay coefficient. τ defines the ray absorption rate along the direction of ray entering.

(18) $$T(s) = e^{-\int_0^k \tau(t)dt}$$

It describes ray intensity traveling from the edge of data field to s. It is also called opacity .If defining α is opacity for this distance, then:

(19) $$\alpha = 1 - T(s) = 1 - e^{-\int_0^k \tau(t)dt}$$

Ray absorption model is widely used in medical image visualization, particularly in CT and MRI data visualization.

The key of ray casting algorithm based on GPU is to complete the sampling, interpolation used Trilinear interpolation by graphic hardware. And the complex combination computation is done by GPU. This algorithm is first proposed by Krüger. It uses vertex coloring program to compute ray cast parameter. and uses deep testing and block query to complete light integral , which affects the rending speed. Scharsach improved this algorithm. The improved algorithm used GPU ' s fragment coloring program to realize loop, To execute by light integral[19].

Stegmaier proposed obtaining ray cast through rendering volume's bounding boxes surface and writing fragment coloring program to realize GPU ray casting algorithm. Zou Hua proposed off-screen rendering technology based on bounding boxes hierarchy which quickly determined ray casting. The basic idea of this algorithm is: setting the color of the cube's each vertex is numerically equal with its space coordinate, through tri-linear interpolation of graphics hardware, the color of any point on the cube surface (r,g,b) is equal with its space coordinate (x,y,z). According to this idea, the parameter of ray casting is obtained through rendering the front and back surface of volume bounding boxes.

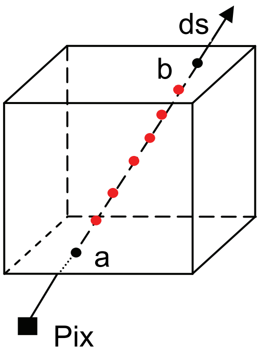

Fig.9. Theory of Ray Casting

According to the parameter of ray casting, carry out integral intensity. Setting ray through 3D volume data field, carry out equal step sampling, and obtain n sampling points. C_i is the NO.i voxel color number, opacity number is a_i ,the color value of voxel is in C_{in}, opacity value is in a_{in} , after ray through this voxel, the color number is C_{out} ,opacity number is a_{out},so:

(20) $$\begin{cases} C_{out}a_{out} = C_{in}a_{in} + C_i a_i(1-a_{in}) \\ a_{out} = a_{in} + a_i(1-a_{in}) \end{cases}$$

Sampling from the first one point to n point, when a_{out} is 1, the following sampling points are no contribution for image, stop integral, at same time, C_{out} is the color number of correspondence screen point.

Formula (20) is RGBA rendering, its color number and opacity number are computed by transfer function and s_i (s_i is voxel number of i sampling point)

(21) $$\begin{cases} C_i = T_c(s_i) \\ a_i = T_a(s_i) \end{cases}$$

T_c is color transfer function. T_a is opacity transfer function.

(B)Algorithm

Because of the limit of memory space, when the data set is too big to be loaded into video cache, the algorithms mentioned above are unable to process such data set. We propose a rendering technology based on field of view divided only rendering voxel in the field of view.

The main idea is to project the 3-dimensional volume data to world coordinate system. Volume data is divided into the visible and the invisible according to field of view. The visible ones are loaded to graphic memory space to be rendered. The detail is as follows.

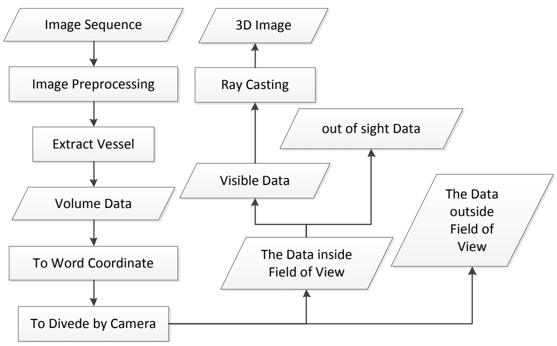

Figure 10. Scene Rendering Program

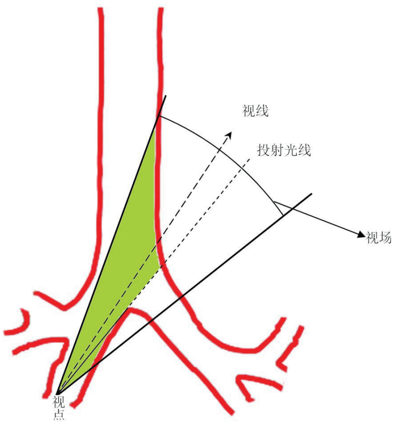

Fig.11. Segmentation for Virtual Vessel

1) load DICOM image sequence, pre-process the raw image, reduce the noise.

2) according to various cavity density of human organ and PCNN segment algorithm, sample lumen pixel data.

3) generate 3-dimensional volume from pixel data of vessel, and project them in world coordinate system.

4) According to the position of virtual camera and its optical angle, we divide 3-dimensional volume into two parts: data inside the vision field and data outside the vision field. No further operation on the latter.

5) According to the visibility, data inside the vision field is again divided into two parts, visible data and invisible data. No operation on invisible data.(how to divide the virtual lumen is shown in Figure11)

6) details of volume rending the visible data are as follows: Formation of the light ray: generate the starting point and the direction of the light ray. Model intersection: give the achivement on intersection detection and the intersection calculation between light and surface Primitive. Rendering and ray derivatives: use of phone light illumination model to calculate and accumulate the value above to the frame buffer relevant pixels. If the light is crossed, the reflection or refraction light can be generated based on the intersection information. if necessary, it will generate a shadow test light.

(C)Results and Analysis

We implement our improved algorithm described above by using VC++6.0 and OpenGL, and the GPU computation is done partly by CUDA. We test the algorithm on three data set, which are from the First Hospital of Jilin University. The configuration of our working computers is Intel Core 2 Duo E6300 CPU, 2GB memory space, GeForceFX 5200 display card, 128MB video memory video cache, Windows XP SP3 system.

The graphic and experimental results are shown in Figure. 12-Figure.14 and in Table 1, respectively.

Table N shows the comparison on activity speed between our algorithm and the traditional volume rendering algorithm.

Fig.12. Bronchus

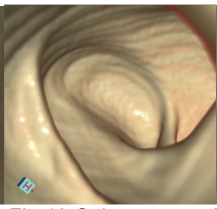

Fig.13.Colon

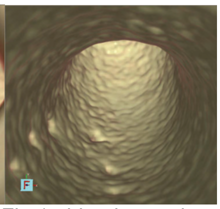

Fig.14.blood vessel

Table 1. Speed Comparison between Traditional Algorithms and Present Algorithm(uint: fps)

CT Image	Bronchus	Colon	blood vessel
Image Extent	512*51*217	512*512*252	512*512*355
Ray casting	9.8	6.4	3.5
Our algorithm	36.2	35.7	32.1

It can be seen from Table 1 that the improved algorithm significantly raised rendering speed. There are two reasons to explain the improvement. One is that bronchia, colons and veins contain a large amount of opacity data; With our algorithm it is no need to consider them. The other is that using GPU's parallel computing from ray generation to rendering clips also saved computer time.

Conclusion

The key technologies such as medical image segmentation, tissue classification and virtual endoscopy scene real-time rendering are not only useful for IGS to improve accuracy and display speed, but also very useful for medical image processing and visualization.

REFERENCES

[1] A D Nijmeh, etal. Image guided navigation in oral and maxillofacial surgery [j]. British Journal of Oral and Maxillofacial Surgery. 2005, 43(4): 294-302.
[2] Luo Xiping,Tian Jie, Lin Yao. An algorithm for Segmentation of Medical Image Series Based on Active Contour Model. Journal of Software. 2002, 13(6): 1050-1058.
[3] Luo Xiping,Tian Jie, Lin Yao. An algorithm for Segmentation of Medical Image Series Based on Active Contour Model. Journal of Software. 2002, 13(6):1050-1058.
[4] Ma Yide,Dai Rolan,Li Lian,et al. Image segmentation of embryonic plant cell using pulse-coupled neural networks[J]. Chinese Science Bulletion, 2002,47(02):167-172.
[5] Ma Yide, Dai Rolan, Li Lian, et al. The State and Development of Cell Image Segmentation Technology. Journal of Biomedical Engineering. 2002,19(3):487-492.
[6] Eckhorn R, Reitboeck H J, Arndt M, Dicke P. Feature linking via synchronization among distributed assemblies: simulation of results from cat cortex. Neural Computation, 1990, 2(3), 293-307.
[7] Robert S. The Tsallis entropy of natural information[J]. Physica A: Statistical Mechanics and Its Applications, 2007, 386(1):101-118.
[8] Tsallis C, Plastino A R, Zheng W M. Power-law sensitivity to initial conditions-new entropic representation[J]. Chaos Solitons and Fractals. 1997, 8(6):885-891.
[9] Eckhorn R,Frien A, Bauer R, et al. . High frequency oscillations in primary visual cortex of awake monkey. NeuroReport, 1993, 4(3):243-246.
[10] Johnson L J, Padgett M L. PCNN models and applications. IEEE Transactions on Neural Networks, 1999, 10(3):480-498.
[11] Stewart R D, Fermin I,Opper M. Region growing with pulse-coupled neural networks: An alternative to seeded region growing[J]. IEEE Transaction on Neural Networks, 2002, 13(6): 1557-1562.
[12] Xiaodong Gu. A New Approach to Image Authentication Using Local Image Icon of Unit-linking PCNN. The 2006 IEEE International Joint Conference on Neural Network. 2006,2:1036-1041.
[13] Jiuwen Zhang,Kun Zhan, Yide Ma. Rotation and Scale Invariant Antinoise PCNN Features for Content-based Image Retrieval. 2007,17(2):121-132.
[14] Yide Ma, Zhaobin Wang,Chenhu Wu. Feature Extraction from Noisy Image Using PCNN. 2006 International Conference on Information Acquisition(ICIA 2006). 2006, 2:808-813;
[15] Zhang Yudong, Wu Lenan. Image Segmentation Based on 2D Tsallis Entropy with Improved Pulse Coupled neural Networks. Journal of Southeast University. 2008,38(4):579-584.
[16] Kaufman A , Mueller K1 Volume visualization and volume graphics [R]1 Stony Brook , NY: Stony Brook University , 2003.
[17] Jens Krüger, Rüdiger Westermann. Linear algebra operators for GPU implementation of numerical algorithms[J]. ACM Trans Graph. 2003, 22(3):908-916.
[18] Scharsach H. Advanced GPU raycasting [C]. Proceedings of Central European Seminar on Computer Graphics 2005, Budmerice Castle, 2005:69-76.
[19] Shi Weili, Miao Yu, Chen Zhanfang, Zhang Hongbiao. Research of Automatic Medical Image Segmentation Algorithm Based on Tsallis Entropy and Improved PCNN. Proceedings of the IEEE International Conference on Mechatronics and Automation.2009:1004-1008.
[20] Shi Weili,MIoa Yu, etc. Real-time Rendering Algorithm for Virtual Endoscopy Based on GPU.ICEEE2010. 2010,No.5,3356-2259.

***Authors**: Lecturer,Shi Weili, Address: School of Computer Science and Technology, 7089 Weixing Road, Changchun 130022, China., E-mail: shiweili@cust.edu.cn;Prof., Li Yanfang, Address: School of Computer Science and Technology, 7089 Weixing Road, Changchun 130022, China., E-mail: lyf@cust.edud.cn ;Lecturer, Miao Yu, Address: School of Computer Science and Technology, 7089 Weixing Road, Changchun 130022, China., E-mail: custmiao@126.com;Master's, Hu Yinlong, Address: School of Computer Science and Technology, 7089 Weixing Road, Changchun 130022, China., E-mail: 458932237@qq.com.*